I. DOBOSZ[*], W. GUMOWSKA[*], M. CZAPKIEWICZ[**]

MAGNETIC PROPERTIES OF Co-Fe NANOWIRES ELECTRODEPOSITED IN PORES OF ALUMINA MEMBRANE

WŁASNOŚCI MAGNETYCZNE NANODRUTÓW Co-Fe OTRZYMANYCH W PROCESIE ELEKTROOSADZANIA W PORACH MEMBRANY TLENKU GLINU

The nanowires of Co_{66}-Fe_{34} alloy were obtained in the process of the electrodeposition in the pores of alumina membrane. With the use of the X-ray diffraction analysis the structure of cobalt-iron alloy wires was determined. The wires have the regular Body Centred Cubic structure (BCC). The influence of membrane parameters, an external magnetic field, and the annealing temperature on the magnetic properties of alloy wires was investigated. The obtained nanowires show a high shape anisotropy in the direction perpendicular to the membrane surface of anodic alumina. It was found that the highest influence on the magnetic properties of the wires has their geometry (height, diameter, and the distance between them). The use of an external magnetic field directed perpendicular to the sample surface during the electrodeposition process and additional thermal treatment (annealing) causes a slight increase of the coercive field, remanence, and volume energy density.

Keywords: Anodic alumina membrane, hysteresis loop, cobalt-iron alloy, nanowires

Nanodruty stopu $Co_{66}Fe_{34}$ uzyskano w procesie elektroosadzania w porach membrany tlenku glinu. Przy pomocy dyfrakcyjnej analizy rentgenowskiej określono strukturę drutów stopu kobalt –żelazo. Druty wykazują strukturę regularną przestrzennie centrowaną (RPC) (ang. BCC). Zbadano wpływ parametrów membrany, zewnętrznego pola magnetycznego oraz temperatury wyżarzania na własności magnetyczne drutów stopowych. Uzyskane nanodruty wykazują wysoką anizotropię kształtu w kierunku prostopadłym do powierzchni membrany anodowego tlenku glinu. Stwierdzono, że największy wpływ na własności magnetyczne ma geometria drutów (wysokość, średnica oraz odległości między nimi). Zastosowanie zewnętrznego pola magnetycznego w kierunku prostopadłym do powierzchni próbki podczas procesu elektroosadzania oraz dodatkowej obróbki termicznej (wyżarzania) powoduje niewielki wzrost pola koercji, remanencji oraz gęstości objętościowej energii.

1. Introduction

The progressive miniaturization of electronic elements and the concurrent increase of the demand for their better and better performance affect the development of research studies in the informatics technology (IT). Nanostructured magnetic materials are used not only in the informatics technology and for the storage of electronic data but also in many other domains such as medicine, automotive industry, environmental protection engineering, and sensor and catalysis technology.

Nanowires are used as the materials for the manufacture of magnetic data storage [1, 2], biomedical materials, sound and/or gas sensors [3-5], and also for the production of diodes and transistors for electronic systems [6].

An anodic alumina membrane is a convenient matrix for the production of nanowires due to the high density of pores and their regular distribution [7, 8]. Besides, anodic alumina is featured by high mechanical strength and thermal stability [8]. The metals which have magnetic properties, as Fe, Co, and Ni and their alloys can be built into the pores of anodic alumina membrane in the process of cathodic deposition from the solutions of the various composition. This way the nanowires made of metals or alloys are obtained.

Nanowire magnetic properties can be formed, among other things, by the selection of pores of appropriate diameters, the distance between pores in the alumina matrix, as well as by the choice of suitable electrodeposition conditions. Another method for changing metal magnetic properties is the selection of a metal of the highest saturation magnetization M_s. From this point of view the nanowires of Co-Fe alloy (M_s = 2.4 T) [9] seem to be exceptionally convenient in comparison with the nanowires made of pure Fe (M_s = 2.2 T) [2, 9] or Co (M_s = 1.8 T). The application of thermal treatment may also result in the improvement of the magnetic properties of nanowires.

An external homogeneous magnetic field applied during the electrodeposition process may also form magnetic properties of Co-Fe wires. The influence of the magnetic field on the electrochemical processes has been observed during the deposition of such metals as Co, Fe, Ni, and their alloys on

---
[*] AGH, UNIVESITY OF SCIENCE AND TECHNOLOGY, FACULTY OF NON – FERROUS METALS, AL. A. MICKIEWICZA 30, 30-059 KRAKÓW, POLAND

[**] AGH, UNIVESITY OF SCIENCE AND TECHNOLOGY, FACULTY OF COMPUTER SCIENCE, ELECTRONICS AND TELECOMUNICATIONS, AL. A. MICKIEWICZA 30, 30-059 KRAKÓW, POLAND

flat electrode [10-20]. Relatively few studies have been carried out to investigate the influence of the magnetic field on the magnetic properties during the deposition of a ferromagnetic metal on the porous membrane surface [21, 22].

The electrodeposition in the magnetic field affects the surface morphology and the crystalline structure of the deposits obtained on a flat electrode. These changes are attributed to the macroscopic magnetohydrodynamic convection (MHD) caused by the Lorentz force [10]. The magnetohydrodynamic effect is a phenomenon affecting the motion of fluid during the process of the electrolytic deposition of metal by forcing the mixing of the electrolyte which may result in changing the morphology and the crystalline structure of the deposit [14, 15].

As for the electrode with high porosity the influence of the MHD effect on the morphology of wires may be different. The fluid motion inside pores induced by the action of the applied magnetic field may not be stationary. Such conditions may give rise to the forming of additional turbulences and forces, totally changing the deposit morphology [21, 22].

Another known phenomenon occurring with the application of the external magnetic field during the metal electrodeposition is the magnetocrystalline effect. The magnetocrystalline effect consists in the change of the structure when an external magnetic field is applied. In the present study, an attempt to investigate the influence of the magnetic field on the magnetic properties of Co-Fe wires has been undertaken.

2. Experiment

The aluminium composition and the detailed information about the process of the preparation of samples for the anodic oxidation process have been presented in the previous papers [23, 24]. The process of anodic oxidation was carried out in two stages. The anodic alumina was formed at a constant voltage in the solutions: 0.3 M sulfuric acid (VI) in the temperature 1°C; 0.3 M oxalic acid in the temperature 2°C; 0.17 M phosphoric acid (V) in the temperature minus 1°C. The time of the first anodizing for the both sulfuric and oxalic acid solutions was 24 hours, whereas for the orthophosphoric acid – 2 hours. After the first anodizing stage, the oxide film was removed by immersing the samples into the solution of the composition: 0.6 M H_3PO_4; 0.2 M CrO_3, in the temperature 80°C for 2 hours. After removal of the oxide film, the samples were subjected to the second anodizing stage under the same conditions as during the first one. The time of the anodizing oxidation process affects the thickness of the oxide films. The second anodizing process for the solutions of sulfuric, oxalic, and orthophosphoric acids lasted for 3, 6, and 10 hours, respectively. After the two anodizing stages, the aluminium substrate was removed in the mixture of the 0.2 M HCl and 0.1 M $CuCl_2$ solution in order to open pores. The barrier layer on the sample bottom was etched in 0.86 M H_3PO_4 in the temperature 30°C. After removal of both the aluminium and the barrier layer, a thin film of gold was sprayed onto the sample surface from the side of the open pores in order to provide an electric contact during the process of the electrodeposition of nanowires. In the areas from which the aluminium substrate was removed, a film of cooper was deposited by means of

electrolysis in potentiostatic conditions. The diagram of the electrolyzer used in the experiment and the methodology of the preparation of the membrane is provided in detail in the previous paper [23].

The alumina membranes of nanoporous and ordered structure with defined pore dimensions (diameter, height, distance between them) were obtained. During the electrolysis process, the Co-Fe alloy was deposited cathodically in the pores of the obtained membranes. The process carried out from sulfate solutions of the composition: 0.5 M $CoSO_4$; 0.3 M $FeSO_4$; 0.3 M H_3BO_3; 0.25 M $C_6H_8O_6$. The pH value of the solution was 3 and it was controlled by adding sulfuric acid (VI) or sodium hydroxide. All experiments were carried out in the room temperature in the three-electrode system, where as a reference electrode a saturated calomel electrode was used (SCE, 0,241 V vs. SHE). All the potentials were recorded in relation to the SCE electrode, and then converted and presented with reference to the standard hydrogen electrode (SHE). A platinum plate used as the counter electrode. The area of the working electrode surface was 0.785 cm^2. The experiment was carried out with "Autolab" potentiostat. The potential was selected on the basis of the chronoamperometric and cycling voltammetry experiments, and it was -0.8 V (vs. SHE)[13].

During the process of the cathodic deposition of Co-Fe alloy nanowires in the magnetic field, the HV7 Walker Scientific electromagnet was used. The experiment was conducted in a homogenous external magnetic field of the strength 0.7 T parallel to the electrode surface. The morphology of the oxide films and their cross-sections were observed with the use of the high resolution scanning microscopy technique with the field emission. The scanning microscope (HITACHI S-4700) was equipped with an EDS system for the chemical composition analysis (NORAN VANTAGE). Structural studies was carried out with the use of the X-ray diffractometer (BRUKER AXS "Discover 8") and filtered $Cu_{K\alpha}$ radiation. The investigation of the magnetic hysteresis loop and its parameters (coercivity, saturation field, saturation magnetization and the remanence) was conducted with the use of the Resonance Vibrating Sample Magnetometer (R-VSM) in the magnetic field directed both perpendicular and parallel to the wire axis.

3. Results

The influence of the electrodeposition time on the height of Co-Fe wires

The electrodeposition of Co-Fe nanowires was carried out in the membrane pores of the following dimensions: the diameter of the pores D_p = 100 nm, the distance between the pores D_c = 250 nm. During the electrodeposition process, different electrolysis times were applied: 2.5, 5, 10, 15, and 30 minutes. The potential was kept constant and it equal -0.8 V (vs. SHE). The relationship between the height (L) of the obtained nanowires and electrodeposition time (t) is shown in Fig. 1. The results obtained in the measurements show that the height of the Co-Fe nanowires is a linear function of time and can be described with the formula (1):

$$L = 0,037 + 0,26 \cdot t \tag{1}$$

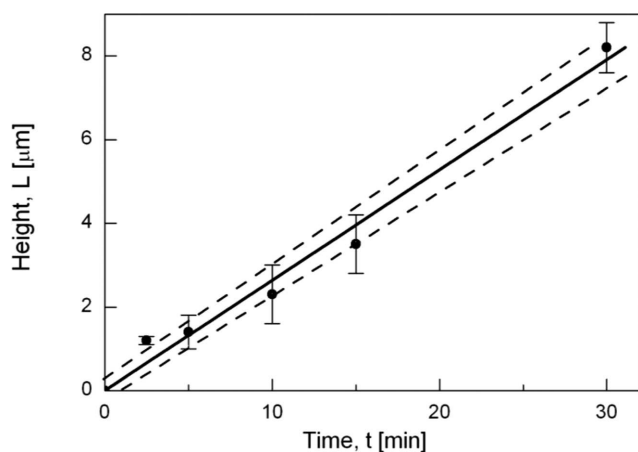The correlation coefficient amounts to 0.989.

Fig. 1. Influence of the electrodeposition time on the height of the Co-Fe wires. Dimensions of the membrane pores: $D_p = 100$ nm, $D_c = 250$ nm, composition of the solution: 0.5 M $CoSO_4$+ 0.3 M $FeSO_4$+ 0.3 M H_3BO_3+ 0.25 M $C_6H_8O_6$

The obtained materials were observed with the use of the scanning microscopy technique. Fig. 2 shows an exemplary photo of the Co-Fe alloy nanowires deposited in the pores of the Al_2O_3 membrane (the height of the nanowires L = 2.5 μm).
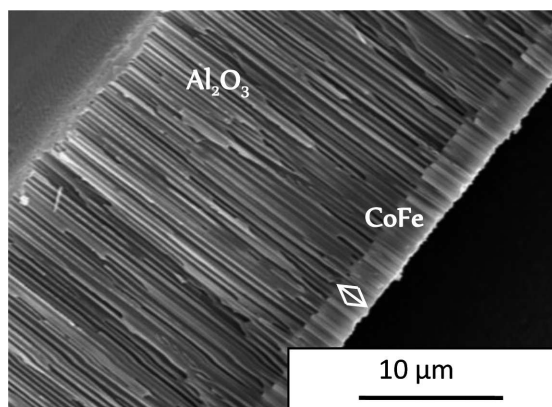

Fig. 2. A SEM microphoto of the Co-Fe wires deposited in the pores of membrane with the dimensions: $D_p = 200$ nm, $D_c = 300$ nm in the solution: 0.5 M $CoSO_4$+ 0,3 M $FeSO_4$+ 0.3 M H_3BO_3+ 0.25 M $C_6H_8O_6$ in the potential -0,8 V (vs. SHE). The height of the Co-Fe wires was about 2.5 μm

The SEM investigation shows that the formation of wires starts in the lower part of the Al_2O_3 membrane. The nanowires are built in uniformly and their height, in the constant potential of the electrodeposition, depends on the process time.

In order to determine the alloy composition, an analysis of the obtained wires was performed. For the analysis the emission spectrometer with induced plasma (ISP) was used. The composition of the obtained Co-Fe nanowires is: Co = 66.5%, Fe = 33.5% (weight procentage).

The X-ray diffraction analysis was applied to determine the structure of Co-Fe alloy nanowires.

The diffractogram for this alloy is presented in Fig 3. In the diffractogram, clear reflections characteristic for the Co-Fe alloy of the crystallographic indices (100), (200), (211), and (310) can be seen. On the basis of the X-ray analysis it was

found that the Co-Fe alloy of the RPC structure had been built in the pores of the alumina membrane.
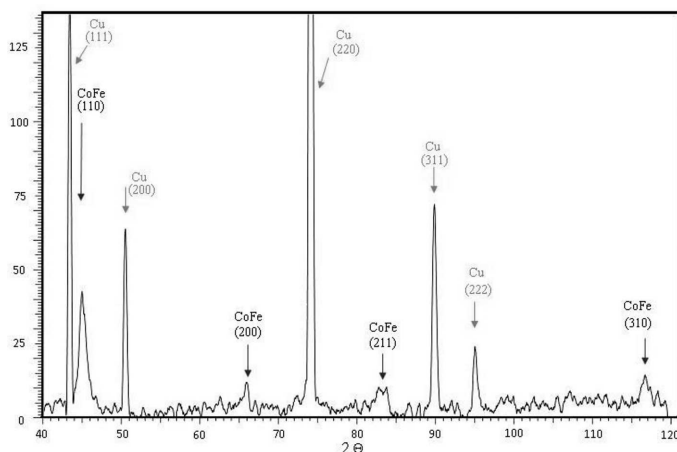

Fig. 3. X-ray phase analysis of the Co-Fe alloy nanowires obtained in the potential -0.80 V (vs. SHE). The peaks characteristic for the alloy and cooper from substrate are described with the indices of crystallographic planes

The magnetic properties of the Co-Fe nanowires of different heights were investigated in the magnetic field directed both perpendicular (I) and parallel (II) to the wire axis with the use of the R-VSM vibration magnetometer. The hysteresis loops are presented as the relationship between the magnetization to saturation magnetization ratio (M/M$_s$) and the magnetic field strength (H).

In Fig. 4 selected magnetization curves for Co-Fe alloy nanowires are presented. In order to investigate the influence of the shape geometry on the magnetic properties of alloy wires, the samples for which the wire height was 1.4, 2.3, 3.5, and 8.2 μm, respectively, were selected.
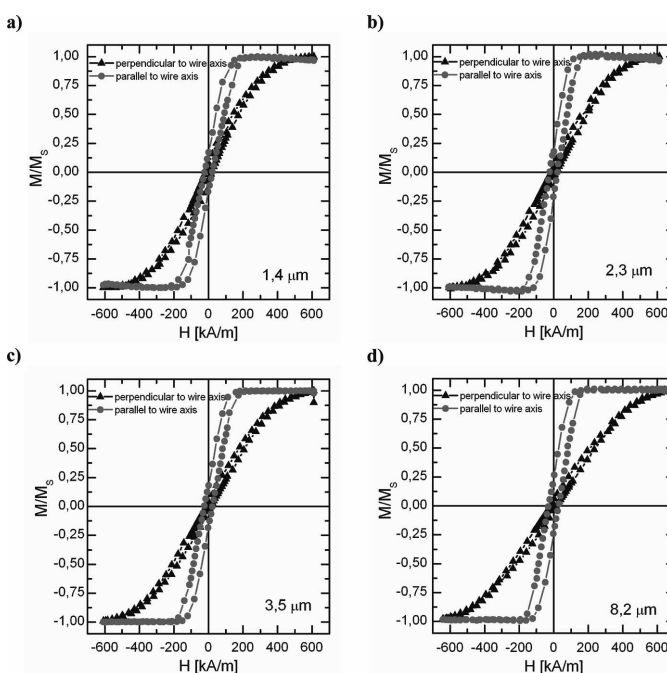

Fig. 4. The hysteresis loops of the cobalt-iron alloy nanowires obtained in the process of the electrodeposition in different times: a) 5, b) 10, c) 15, and d) 30 minutes from the solution of the following composition: 0.5 M $CoSO_4$+ 0.3 M $FeSO_4$+ 0.3 M H_3BO_3+ 0.25 M $C_6H_8O_6$; electrodeposition was conducted at the potential -0,80 V

The values characterizing the magnetic properties of the Co-Fe alloy nanowires of different heights (L)

L [μm]	Remanent energy density $\mu_0 M_r \cdot H_c$ [kJ/m³]		Remanence energy $\mu_0 M_r \cdot H_c \cdot V$ [J]		M_r/M_s		Remanence M_r [emu/cm³]		Coercivity H_c [kA/m]	
	(II)	(⊥)	(II) × 10⁻¹⁶	(⊥) × 10⁻¹⁶	(II)	(⊥)	(II)	(⊥)	(II)	(⊥)
					to wire axis					
1.4	8,6	2,9	0,94 (0,59 keV)	0,32 (0,2 keV)	0,16	0,06	301	130	22,9 (287 Oe)	18,1 (227 Oe)
2.3	10,2	1,5	1,85 (1,15 keV)	0,28 (0,17 keV)	0,18	0,04	356	81	23,0 (288 Oe)	15,3 (192 Oe)
3.5	9,65	1,6	2,64 (1,65 keV)	0,45 (0,28 keV)	0,17	0,03	325	96	23,7 (297 Oe)	13,7 (192 Oe)
8.2	16,1	1,8	10,1 (6,3 keV)	1,13 (0,71 keV)	0,2	0,04	443	84	29,0 (363 Oe)	17,1 (214 Oe)

To carry out a quantitative analysis of the relationship between the magnetization and the magnetic field strength, the following values have been determined or defined:
- magnetic field strength (H),
- magnetization (M),
- coercive field, coersivity (H_c),
- M_r/M_s remanence squareness, where M_r – residual magnetization (remanence), M_s – saturation magnetization,
- volume energy density of remanence $\mu_0 M_r H_c$,
- remanence energy $\mu_0 M_r H_c \cdot V$, where V is nanowires volume.

The values are presented in Table 1.

For the wires of the height 8.2 μm (Fig. 4 d) a clear magnetization anisotropy is observed. The sample demonstrates a privileged magnetization direction along the axis of wires (easy direction), whereas the field direction perpendicular to the axis of wires is the difficult direction. This is confirmed by the evident differences in the remanence energy between the magnetization curves. Along with the decrease of the wire lengths, a decrease of the anisotropy is observed (Fig. 4 a, b, and c).

The relationship between the remanence energy and the height of nanowires is presented in Fig. 5. The remanence energy measured perpendicularly to the sample plane (i.e. parallel to the wire axis) is higher when compared with the energy for the magnetic field in the parallel direction to the sample plane. With the increase of wire length from 1.2 μm up to 8.2 μm, a linear increase from 0.1 keV to about 6 keV of the energy directed perpendicularly to the sample surface is observed. The largest differences of the remanence energy within the sample plane and perpendicularly to it are observed for the longest wires, i.e. 8.2 μm (Fig. 5).

The height of Co-Fe wires significantly affects the magnetic properties. With the increase of the nanowire height both the energy volume density and the shape anisotropy increase (Fig. 5). The easy magnetization direction is oriented along the wire axis.

The simplest description of the interaction of two nanowires comes down to the determination of the demagnetization field (H_z) generated by one of the wires located at the D_c distance from the second one. In accordance with the Kumar's [25] and Sorop's [26] studies, the demagnetization field can be described with the formula:
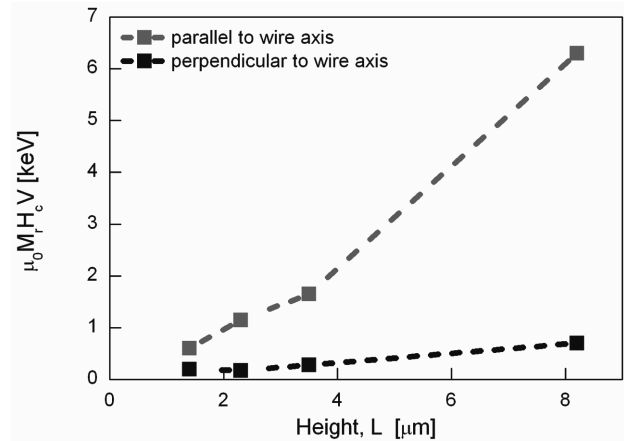

Fig. 5. The relationship between the remanence energy measured parallel and perpendicular to the wire axis and the height of the Co-Fe wires deposited in the membrane of the dimensions D_p = 100 nm, D_c = 250 nm, and the time of the electrodeposition in the solution: 0.5 M $CoSO_4$+ 0,3 M $FeSO_4$+ 0.3 M H_3BO_3+ 0.25 M $C_6H_8O_6$

$$H_z = -\frac{m}{\sqrt[3]{D_c^2 + \frac{L^2}{4}}} \qquad (2)$$

where m is the dipole moment (m = M_sV), and the V – wire volume.

On the basis of Equation (2) the H_z = f(L) graph has been made (Fig. 6).

This relationship has its maximum which corresponds to the highest H_z value in connection with wire heights. The values calculated for the wires obtained in our investigations are marked with points. The maximum value occurs for the wires of the lengths below 1 μm. For the nanowires of the smallest diameter (D_p = 18 nm) the value H_z = 0.3 T, whereas for the nanowires of the largest diameter (D_p = 200 nm) the value H_z = 3.9 T. The demagnetization field (H_z) is formed as the result of the interaction of nanowires and it forces the magnetization (M) of the opposite orientation. Therefore, the lower

the demagnetization field is, the higher is the magnetization. Thus, the Co-Fe wires of the length from 4 up to 9 μm show the highest magnetization value.
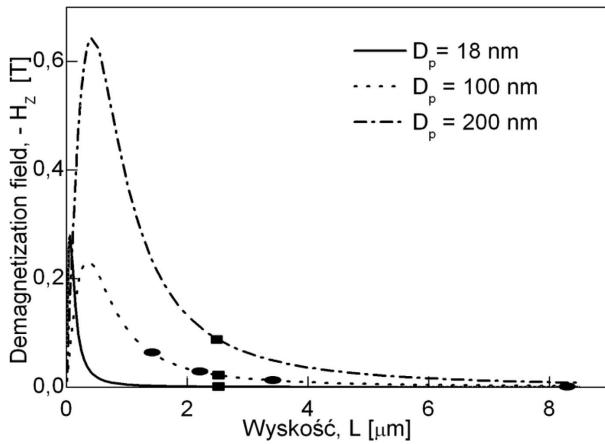

Fig. 6. The influence the demagnetization field (H_z) on the length of the Co-Fe wires deposited in the membranes with the pores of the diameters 18, 100, and 200 nm
■ – wires of the height 2.5 μm (Tab. 3),
● – wires of different heights: 1.4, 2.3, 3.5. and 8.2 μm (D_p = 100 nm, D_c = 250 nm)

The graph illustrating the relationship between the demagnetization field and the wire lengths is results from a model of the magnetostatic interaction between wires and it can be used for the estimate of the interaction influence only. In addition, the H_z value is dependent not only on the height (L) of nanowires, but also on the pore diameters (D_p) and the distance between pores (D_c).

The analysis of the chemical composition (ISP) of the obtained nanowires shows that the alloy composition is as follows: Co – 66.5%, and Fe – 33.5% [weight percentage]. The X-ray phase analysis (Fig. 3) indicates that the structure is of the Body Centred Cubic (BCC) type for which the magnetocrystalline anisotropy is negligible small [27]. This means that the magnetization direction mainly on the shape anisotropy, therefore on the length and the diameter of wires as well as the distance between them. That is why even for

relatively short wires (3.5 μm) a clear anisotropy along the wire axis is observed.

Besides, for the nanowires of Co-Fe alloy the anisotropy energy along the nanowire axis is sufficiently high (in comparison with the coupling energy between neighbouring wires) to provide a domination of the easy direction along the wire axis within the investigated height range.

The influence of the external magnetic field used in the process of the electrodeposition on the magnetic properties of Co-Fe alloy wires

In the process of the electrodeposition of alloy, the magnetic field (0.7 T) directed perpendicularly ($\perp$) to the sample surface was applied. An Al_2O_3 membrane with the pores of the diameter 70 nm distanced by 100 nm was used. The electrodeposition time was constant and it amounted to 5 minutes. The Co-Fe alloy wires of height about 7 μm were obtained in the magnetic field perpendicular to the sample surface and without any magnetic field, respectively. The hysteresis loops are shown in Fig. 7.
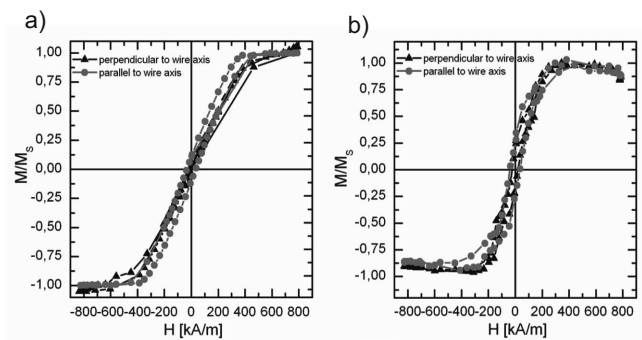

Fig. 7. The hysteresis loops for the Co-Fe alloy nanowires obtained in the solution: 0.5 M $CoSO_4$+ 0.3 M $FeSO_4$+ 0.3 M H_3BO_3+ 0.25 M $C_6H_8O_6$ in the potential -0,8 V: a) without magnetic field, b) in an external magnetic field 0.7 T – perpendicular to the sample surface

The characteristic values for the magnetic field are presented in the Table 2.

TABLE 2

The values characterizing the magnetic properties of the Co-Fe alloy nanowires obtained without and with the application of external magnetic field of strength 0.7 T in the configuration of the field perpendicular to the membrane surface. The height of the nanowires L = 7 μm

Configuration	Remanent energy density $\mu_0 M_r \cdot H_c$		Remanence energy $\mu_0 M_r \cdot H_c \cdot V$		M_r/M_s		Remanence M_r		Coercivity H_c	
	[kJ/m^3]		[J]				[emu/cm^3]		[kA/m]	
	(II)	($\perp$)	(II) $\times 10^{-16}$	($\perp$) $\times 10^{-16}$	(II)	($\perp$)	(II)	($\perp$)	(II)	($\perp$)
					to wire axis					
0T	8,3	0,6	2,4 (1,5 keV)	0,18 (0,1 keV)	0,10	0,03	201	52	32,9 (411 Oe)	9,6 (120 Oe)
0,7T $\perp$	23,8	13,9	6,4 (4,0 keV)	3,76 (2,35 keV)	0,28	0,21	541	399	35,2 (440 Oe)	28,0 (350 Oe)

For the Co-Fe wires deposited without magnetic field, a slight magnetic anisotropy can be observed. The difference between the hysteresis loops in the field perpendicular to the wire axis and the field parallel to it is small.

The application of the external magnetic field of strength 0.7 T in the configuration perpendicular to the membrane surface (i.e. along the wire axis) during the deposition of alloy wires slightly affects the changes in magnetic properties. The Co-Fe alloy does not show any privileged magnetization direction.

The influence of the Al_2O_3 membrane parameters on the morphology of Co-Fe wires

The electrodeposition of Co-Fe wires was carried out with the use of membranes, the parameters of which are presented in Table 3.

TABLE 3

The parameters of the membranes used during the electrodeposition of Co-Fe alloy

Electrolyte	D_p [nm]	D_c [nm]	L [μm]
0,3 M H_2SO_4	18	41	
0,3 M $H_2C_2O_4$	100	250	2,5
0,17M H_3PO_4	200	300	

In order to minimize the influence of the dipolar coupling between neighbouring wires, the height of the wires was kept constant and amounted to 2.5 μm.

Fig. 8 shows the magnetization curves for the Co-Fe alloy nanowires deposited in these membranes.

In Table 4, the values characterizing the magnetic field of the investigated nanowires are presented.

Along with the increase of pore diameters, a clear decrease of the coercive field, the remanence, and the remanence energy is observed in the magnetic field directed parallel to the wire axis.

The wires of the smallest pore diameters (Fig. 8 a) do not show the typical hysteresis in both perpendicular and parallel direction to the wire axis. A co-existence of both easy and

difficult magnetization axis can be observed. This can be seen in the fields perpendicular and parallel to the wire axis. For the field $\perp$ to the wire axis (in the membrane plane) a small coercive field is observed.

Along with the increase of the wire diameters (D_p) from 18 nm up to 100 nm, the effect of the anisotropy changes: the wire axis is the one of easy magnetization, whereas the field direction perpendicular to the wire axis is the difficult direction (Fig. 8 b).

The further increase of the wire diameters up to 200 nm (Fig. 8 c) leads to the disappearance of the hysteresis in both directions; the remanence value is small.

The reduction of the coercive field, the remanence, and the remanence squareness M_r/M_s for Co-Fe alloy wires was also observed by Khan and Petrikowski [22].
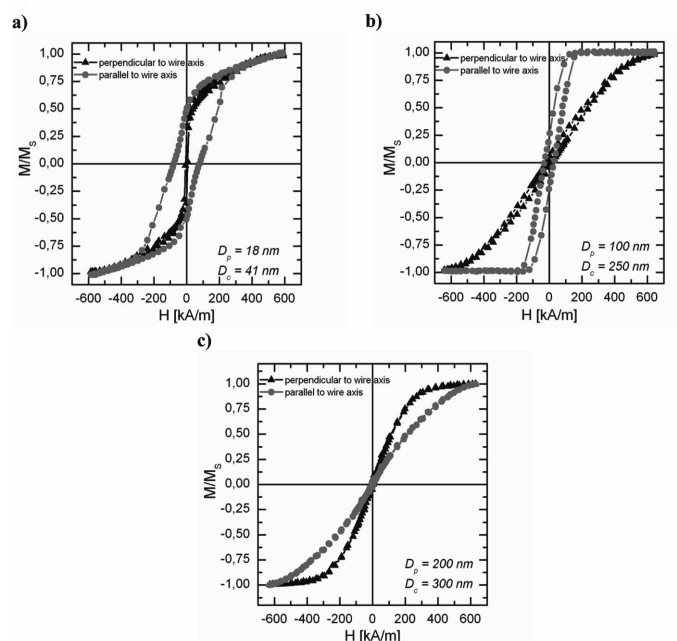

Fig. 8. The hysteresis loops for the Co-Fe alloy nanowires of the diameters: a) 18 nm, b) 100 nm, and c) 200 nm obtained from the solution: 0.5M $CoSO_4$ + 0,3M $FeSO_4$ + 0.3M H_3BO_3 + 0.25M $C_6H_8O_6$; electrodeposition in the potential -0.80 V; the height of wires about 2.5 μm

TABLE 4

The values characterizing the magnetic properties of the Co-Fe alloy nanowires obtained by the electrodeposition in the alumina membrane of different parameters: L = const. = 2.5 μm

D_p, D_c [nm]	Remanent energy density $\mu_0 M_r \cdot H_c$ [kJ/m^3] (II)	($\perp$)	Remanence energy $\mu_0 M_r \cdot H_c \cdot V$ [J] (II) $\times 10^{-16}$	($\perp$) $\times 10^{-16}$	M_r/M_s (II)	($\perp$)	Remanence M_r [emu/cm^3] (II)	($\perp$)	Coercivity H_c [kA/m] (II)	($\perp$)
					to wire axis					
18, 41	92,4	4,3	0,59 (0,37 keV)	0,03 (0,02 keV)	0,5	0,28	950	553	77,8 (973 Oe)	6,2 (78 Oe)
100, 250	10,2	1,5	1,85 (1,15 keV)	0,28 (0,17 keV)	0,18	0,04	356	81	23,0 (288 Oe)	15,3 (192 Oe)
200, 300	0,39	0,48	0,30 (0,19 keV)	0,37 (0,23 keV)	0,02	0,04	46	70	6,7 (84 Oe)	5,5 (96 Oe)

The influence of the annealing process on the magnetic properties of Co-Fe nanowires

Co-Fe alloy nanowires were subjected to an annealing treatment in the temperature 100, 200, 400, and 500°C. The annealing process was carried out in the argon atmosphere. For the thermal treatment the wires deposited in the membrane pores of the diameter D_p = 200 nm, distanced by 300 nm, and of the height 2.5 μm were selected. Fig. 9 shows the obtained hysteresis loops.
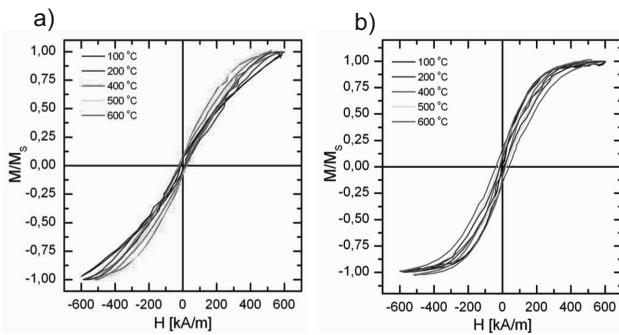

Fig. 9. The hysteresis loops for the Co-Fe wires of the dimensions D_p = 200 nm, D_c = 300 nm obtained from the solution 0.5 M $CoSO_4$ + 0.3 M $FeSO_4$ + 0.3M H_3BO_3 + 0.25M $C_6H_8O_6$ subjected to the thermal treatment in the temperatures from 100 up to 600°C. The investigation was carried out in the magnetic field directed: a) perpendicular, and b) parallel to the membrane surface

In Fig. 9 the collective magnetization curves for the magnetic field directed perpendicular to the sample surface (Fig. 9 a) and parallel to it (Fig. 9 b) annealed in the temperature from 100 up to 600°C are presented. The course of these relationships shows that the increase of the annealing temperature clearly affects the increase of the coercive field in the magnetic field in both magnetization directions.

In Table 5 the values characterizing the magnetic properties are presented.

The CoFe wires of the diameter 200 nm and the height 2.5 μm annealed in the temperature 100°C do not show any hysteresis. There is no easy magnetization axis. By increasing

the annealing temperature up to 400°C, a slight increase of the remanence energy, the volume energy density, and an increase of the anisotropy perpendicular to the wire axis occurs. This direction is determined by the shape anisotropy resulting from the dimensions of alloy wires. The further increase of the annealing temperature above the allotropic transformation temperature (417°C) leads to the increase of the remanence energy with a simultaneous decrease of the magnetization anisotropy.

The increase of the coercive field due to the annealing treatment is probably connected with the change of the microstructure in the annealing process. During the cathodic reduction of Fe^{2+} and Co^{2+} ions in relatively low potential (-0.8 V) some internal stresses may occur that may effect in the decrease of the values of both the coercive field and the remanence. Along with the increase of the annealing temperature, the saturation magnetization (M_s) increases, and thereby also the coercive field. This is confirmed by the obtained results. On the other hand, there is a big difference between the coefficient of thermal expansion between the Co-Fe alloy (α_{CoFe} = 14.0 × 10^{-6} K^{-1}) and alumina ($\alpha_{Al_2O_3}$ = 6.0 × $10^{-6}K^{-1}$). The wires of Co-Fe alloy expand along the wire axis and may form a structure characterized by an easy axis perpendicular to the sample surface. This may affect the change of the anisotropy, which increases during the process of annealing in the temperature 600°C. Then, at higher temperatures iron atoms in the alloy wires will react with the oxygen present in the alumina membrane, and this is conducive for the formation of iron oxides or other paramagnetic compounds ($FeAl_2O_4$ and α- ($Fe_xAl_{1-x})_2O_3$) [28, 29] which may lower the saturation magnetization and affect the change of the magnetization anisotropy.

4. Conclusions

From among the obtained Co-Fe alloys the longest (8.2 μm) alloy nanowires are featured by the highest magnetic anisotropy appropriate for magnetic recording purposes. Short wires (1.4 μm) are characterized by a similar, low remanence energy and low M_r/M_s remanence squareness in both direc-

TABLE 5

The values characterizing the magnetic properties of Co-Fe alloy nanowires annealed in different temperatures

t^o [°C]	Remanent energy density $\mu_0M_r \cdot H_c$ [kJ/m³]		Remanence energy $\mu_0M_r \cdot H_c \cdot V$ [J]		Remanence M_r [emu/cm³]		Coercivity H_c [kA/m]	
	(II)	($\perp$)	(II) × 10^{-16}	($\perp$) × 10^{-16}	(II)	($\perp$)	(II)	($\perp$)
			to wire axis					
100	1,5	1,8	0,14 (0,09 keV)	0,17 (0,11 keV)	102	209	12 (150 Oe)	6,9 (86 Oe)
200	1,2	2,2	0,12 (0,07 keV)	0,21 (0,13 keV)	73	132	13,6 (170 Oe)	13,6 (170 Oe)
400	2,6	4,5	0,25 (0,15 keV)	0,42 (0,26 keV)	113	221	18,5 (231 Oe)	16,2 (203 Oe)
500	3,9	5,7	0,37 (0,23 keV)	0,53 (0,33 keV)	132	192	23,7 (296 Oe)	23,7 (296 Oe)
600	4,9	14,7	0,46 (0,29 keV)	1,39 (0,87 keV)	163	336	23,9 (299 Oe)	35,2 (440 Oe)

tions: parallel and perpendicular to the wire axis. This means that the magnetic anisotropy is low.

For Co-Fe wires, the magnetocrystalline anisotropy is very weak, whereas a significant role plays the shape anisotropy and the mutual dipolar interaction between wires. The diffraction analysis of Co-Fe wires indicates the presence of the Co-Fe phase of the Body Centred Cubic (BCC) lattice with a strong reflection originated from the phase (110).

The application of the external magnetic field in the direction perpendicular to the sample surface during the process of the cathodic reduction of Co^{2+} and Fe^{2+} ions causes an increase of the coercive field, the remanence, and the volume energy density of Co-Fe alloys.

The value which plays a significant role is the demagnetizing field (H_z), which determines in large measure the magnetic behaviour of alloy wires. The maximum value of the demagnetization field the alloy wires may reach depends on their diameters and the distance between them, and it increases with the increase of wire length.

The annealing of wires in the temperature range from 100 up to 400°C causes a slight increase of the anisotropy in the direction perpendicular to the wire axis. This direction is determined by the shape anisotropy resulting from the wire dimensions. The further increase of the annealing temperature above the allotropic transformation temperature (417°C) leads to the increase of the remanence energy with a concurrent decrease of the magnetization anisotropy.

The increase of both the diameter of Co-Fe alloy wires and the distance between them significantly affects the magnetic properties. With the increase of the wire diameters the reduction of coercive field, the volume energy density, and the remanence is observed.

Summarizing, the magnetic properties of Co-Fe nanowires depend mainly on their height, diameter, and the distance between them. These factors can be controlled by the selection of the Al_2O_3 membrane parameters (pore diameters and the distance between them) as well as the potential and the electrodeposition time.

Acknowledgements

REFERENCES

[1] D.J. S e l l m y e r, H. Z e n g, M. Y a n, S. S u n, Y. L i u, Handbook of Advanced Magnetic Materials. IV: Properties and Application, 2006.

[2] D. S e l l m y e r, M. Z h e n g, R. S k o m s k i, Magnetism of Fe, Co and Ni nanowires in self- assembled arrays, Journal of Physics: Condensed Matter 13, R433 (2001).

[3] M. H e r n á n d e z - V é l e z, Nanowires and 1D arrays fabrication: An overview, Thin Solid Films 495, 51 (2006).

[4] P.D. M c G a r y, L. T a n, J. Z o u, B.J.H. S t a d l e r, Magnetic nanowires for acoustic sensors, Journal of Applied Physics 99, 08B310 (2006).

[5] M. Y u n, N.V. M y u n g, R.P. V a s q u e z, J. W a n g, H. M o n b o u q u e t t e, Nanowire growth for sensor arrays, Proceedings of the SPIE 5220, 37 (2003).

[6] Y. C u i, C.M. L i e b e r, Functional nanoscale electronic devices assembled using silicon nanowire building blocks, Science 291, 85, 1 (2001).

[7] A. S u g a w a r a, D. S t r e b l e c h e n k o, M. M c - C a r t n e y, M.R. S c h e i n f e i n, Magnetic coupling in self-organized narrow-spaced Fe nanowire arrays, IEEE Transactions on Magnetics 34, 1081 (1998).

[8] D. R o u t k e v i t c h, A.A. T a g e r, J. H a r u y a m a, D i y a a A l m a w l a w i, M. M o s k o v i t s, J.M. X u, Non-lithographic nano-wire arrays: fabrication, physics and device applications, IEEE Transaction on Magnetism 43, 1646 (1996).

[9] J. W a n g, X. Z h o u, Q. L i u, D. X u e, F.S. L i, B. L i, Magnetic texture in iron nanowire arrays, Nanotechnology 15, 485 (2004).

[10] J.A. K o z a, S. M ü h l e n h o f f, M. U h l e m a n n, K. E c k e r t, A. G e b e r t, L. S c h u l t z, Desorption of hydrogen from an electrode surface under influence of an external magnetic field – In-situ microscopic observations, Electrochemistry Communications 11, 425 (2009).

[11] A. K r a u s e, M. U h l e m a n n, A. G e b e r t, L. S c h u l t z, The effect of magnetic fields on the e-lectrodeposition of Co and Cu, Electrochimica Acta 49, 4127 (2004).

[12] H. M a t s u s h i m a, Y. F u k u n a k a, H. Y a s u d a, S. K i k u c h i, Phenomenological discussion of Fe and Co film electrodeposited in a magnetic field, ISIJ International 45, 1001 (2005).

[13] I. D o b o s z, Elektrochemiczne metody otrzymywania kompozytów tlenek aluminium – metal (stop) o własnościach magnetycznych. PhD thesis, AGH, Kraków 2011.

[14] A. I s p a s, H. M a t s u s h i m a, W. P l i e t h, A. B u n d, Influence of a magnetic field on the ele-ctrodeposition of nickel – iron alloys, Electrochimica Acta 52, 2785 (2007).

[15] H. M a t s u s h i m a, A. I s p a s, A. B u n d, B. B o z z i m, Magnetic field effects on the initial sta- ges of electrodeposition processes, Journal Electroanalytical Chemistry 615, 191 (2008).

[16] A. I s p a s, A. B u n d, Influence of a magnetic field on the electrodeposition of nickel and nickel-iron alloys, in The 15th Riga and 6th PAMIR Conference on Fundamental and Applied MHD, 135-138 (2011).

[17] M. E b a d i, W.J. B a s i r u n, Y. A l i a s, Influence of magnetic field on the electrodeposition of Ni-Co alloy, Journal of Chemical Society 122, 279 (2010).

[18] P. F r i c o t e a u x, C. R o u s s e, Influence of substrate, pH and magnetic field onto compo- sition and current efficiency of electrodeposited Ni-Fe alloys, Journal of Electroana-lytical Chemistry 612, 9 (2008).

[19] A. I s p a s, H. M a t s u s h i m a, A. B u n d, B. B o z z i n i, A study of external magnetic-field effects on nickel-iron alloy electrodeposition, based on linear and non-linear differential AC electrochemical response measurements, Journal of Electroanalytical Chemistry 651, 197 (2011).

[20] A. I s p a s, H. M a t s u s h i m a, A. B u n d, B. B o z z i n i, Nucleation and growth of thin nickel layers under the influence of a magnetic field, Journal of Electroanalytical Chemistry 626, 174 (2009).

[21] J. S á n c h e z - B a r r i g a, M. L u c a s, G. R i v e r o, P. M a r i n, A. H e r n a n d o, Magnetoelectrolysis of Co nanowire arrays grown in a track-etched polycarbonate membrane, Journal of Magnetism and Magnetic Materials 312, 99 (2007).

[22] H.R. K h a n, K. P e t r i k o w s k i, Synthesis and properties of the arrays of magnetic nano- wires of Co and CoFe, Materials Science and Engineering C 19, 345 (2002).

[23] W. Gumowska, I. Dobosz, M. Uhlemann, J.A. Koza, Al_2O_3 – Co and Al_2O_3 – Fe composites obtained by the electrochemical method, Archives of Metallurgy and Materials **54**, 1119 (2009).

[24] I. Dobosz, W. Gumowska, M. Uhlemann, J.A. Koza, Al_2O_3 –Co and Al_2O_3 –Fe composites obtained by the electrochemical method.Part II. Magnetic properties of Co and Fe nano-wires, Archives of Metallurgy and Materials **55**, 684 (2010).

[25] A. Kumar, S. Fähler, H. Schlörb, K. Leistner, L. Schultz, Competition between shape anisotropy and magnetoelastic anisotropy in Ni nanowires electrodeposited within alumina templates, Physical Reviev B **73**, 064421 (2006).

[26] T.G. Sorop, K. Nielsch, P. Göring, M. Kröll, W. Blau, R.B. Wehrspohn, U. Gösele, L.J.D. Jongh, Study of the magnetic hysteresis in arrays of ferromagnetic Fe nanowires as a function of the template filling fraction, Journal of Magnetism and Magnetic Materials **272 -276**, 1656 (2004).

[27] P.S. Fodor, G.M. Tsoi, L.E. Wenger, Fabrication and characterization of $Co_{1-x}Fe_x$ alloy nanowires, Journal of Applied Physics **91**, 8186 (2002).

[28] A. Jagminas, K. Mažeika, J. Reklaitis, D. Baltrūnas, V. Pekstas, Annealing effects on the transformations of Fe nanowires encapsulated in the alumina template pores, Materials Chemical Physics **115**, 217 (2009).

[29] K. Mažeika, J. Reklaitis, Arunas Jagminas, D. Baltrūnas, Studies of oxidation of iron nanowires encased in porous aluminium oxide template, Hyperfine Interact **189**, 137 (2009).